Two-color rubidium fiber frequency standard

C. Perrella,[1,3,*] P. S. Light,[1,3] J. D. Anstie,[1,3] F. N. Baynes,[1] F. Benabid,[2] and A. N. Luiten[1,3]

[1]School of Physics, University of Western Australia, Perth, Western Australia 6009, Australia

[2]GPPMM Group, Xlim Research Institute, CNRS, Universite de Limoges, France

[3]Institute of Photonics and Advanced Sensing (IPAS) and the School of Chemistry and Physics, The University of Adelaide, Adelaide SA 5005, Australia

*Corresponding author: chris.perrella@adelaide.edu.au

Received December 26, 2012; revised April 20, 2013; accepted May 13, 2013;
posted May 15, 2013 (Doc. ID 182187); published June 11, 2013

We demonstrate an optical frequency standard based on rubidium vapor loaded within a hollow-core photonic crystal fiber. We use the $^5S_{1/2} \rightarrow {}^5D_{5/2}$ two-photon transition, excited with two lasers at 780 and 776 nm. The sum-frequency of these lasers is stabilized to this transition using modulation transfer spectroscopy, demonstrating a fractional frequency stability of 9.8×10^{-12} at 1 s. The current performance limitations are presented, along with a path to improving the performance by an order of magnitude. This technique will deliver a compact, robust standard with potential applications in commercial and industrial environments. © 2013 Optical Society of America

OCIS codes: (060.5295) Photonic crystal fibers; (120.4800) Optical standards and testing; (190.4180) Multiphoton processes.

http://dx.doi.org/10.1364/OL.38.002122

There is a great deal of interest in the development of compact, robust, efficient, and relatively inexpensive atomic frequency standards aimed at commercial and industrial markets, where frequency stabilities in the range of 10^{-10} to 10^{-13} are desired. These devices, based on either optical [1,2] or microwave [3,4] atomic transitions, are aimed at applications such as telecommunication [4] and navigation systems [5]. One such commercial device has achieved a fractional frequency stability of $2.5 \times 10^{-10}\,\tau^{-1/2}$ for integration times of $1 < \tau < 1000$ s [4]. Here, we demonstrate a device that could be of similar size, that outperforms this commercial product by an order of magnitude over short time scales with another order of magnitude in performance through to be achievable. This is achieved through a novel twin approach: first, a hollow-core photonic crystal fiber (HC-PCF) is used in combination with a two-photon transition in rubidium (Rb) and second, exploitation of the energy level structure of Rb to enhance the two-photon transition rate using a two-color excitation technique.

The most stable laboratory-based optical Rb frequency standards utilize the $^5S_{1/2} \rightarrow {}^5D_{5/2}$ two-photon transition and have demonstrated a frequency stability of $3 \times 10^{-13}\,\tau^{-1/2}$ for $1 < \tau < 1000$ s [6,7]. This transition can be excited in a Doppler-free configuration [8], resulting in a linewidth of 334 kHz, limited by the natural lifetime [9] of the $^5D_{5/2}$ state. These standards use a single 778 nm laser tuned to half the energy difference between the $^5S_{1/2}$ and $^5D_{5/2}$ states. To increase the Rb two-photon transition rate, and thereby the potential frequency stability, an optical cavity is typically used to increase the optical power interrogating the transition [6,7]. This makes these clocks complex and fragile devices.

This Letter presents an alternative approach that avoids the complexity of an optical cavity [6,7] through the use of HC-PCF. The geometry of a HC-PCF allows production of high optical intensities, at low input powers, over arbitrary lengths. Such attributes enhance light-atom interactions, improving the signal-to-noise ratio of frequency stabilization signals. Moreover, the flexibility and small volume of HC-PCF makes it an excellent basis for a compact, robust, and efficient high-performance frequency standard.

In our scheme, further enhancement of the two-photon transition is gained over previous work [6,7] by using a two-color excitation technique. Two lasers at 780 and 776 nm were used to drive the two-photon ^{87}Rb $^5S_{1/2}(F = 2) \rightarrow {}^5D_{5/2}(F' = 4)$ transition, seen in Fig 1(a), with a small detuning from the intermediate $^5P_{3/2}$ state. A detuning of $\Delta \approx 2$ GHz was used which, when compared to the single laser 778 nm based standards [6,7] with $\Delta \approx 1$ THz, provided a 10^8 enhancement in transition rate [10]. The two-photon transition displayed a spectral full-width at half-maximum of 10.4 MHz, limited predominantly by transit time broadening in combination with residual Doppler and magnetic field broadening [11]. At typical driving powers used here, the transition

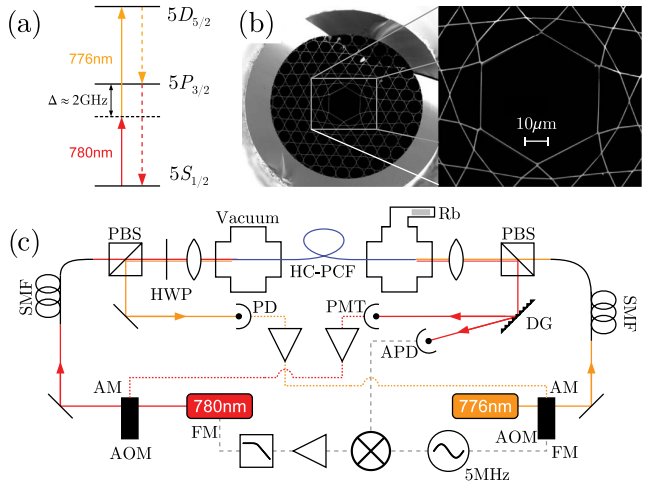

Fig. 1. (a) Two-photon transition energy level diagram. Solid arrows are driving lasers, dashed arrows show decay routes. (b) Scanning electron microscope image of the kagome HC-PCF used. (c) Schematic of the experimental setup. AOM, acousto-optic modulator; SMF, single-mode fiber; HWP, half-wave plate; PBS, polarizing beam splitter; DG, diffraction grating; PMT, photomultiplier tube; PD, photodiode.

exhibited ≈5% absorption of the 780 nm laser within the HC-PCF. In this scheme, neither the 780 nor 776 nm lasers were individually frequency stabilized: it was the sum-frequency of these lasers that was stabilized to the $^5S_{1/2}$ and $^5D_{5/2}$ energy level difference.

Figure 1(c) shows the optical setup used to excite the two-photon transition, along with the electronic feedback systems. The two driving lasers were an extended cavity diode laser at ~780 nm and a titanium:sapphire laser at ~776 nm. The lasers' optical modes were spatially filtered by single mode fibers, and their polarizations were set to be linearly orthogonal, enabling their separation after the HC-PCF. Doppler-free spectroscopy of the two-photon transition was achieved by coupling the lasers into opposite ends of the HC-PCF using 60 mm lenses.

The HC-PCF used had a kagome-style cladding structure [12], shown in Fig 1(b), with a core diameter of 45 μm, which together provided low-loss multimode guidance from 600 to 1600 nm. Observation of the Rb vapor's fluorescence was used to qualitatively measure variations of the Rb density along the length of the fiber. This revealed over half of the 40 cm fiber contained measurable quantities of Rb, although the density decreased along the fiber's length.

After the HC-PCF, the lasers were separated using polarizing beam splitters. A diffraction grating further isolated the 780 nm beam from any residual 776 nm light before detection with an avalanche photodiode.

A frequency discrimination signal was generated using a variant of modulation transfer spectroscopy (MTS) [13]. This was achieved through frequency modulating the 776 nm laser at 5 MHz (modulation depth ~5 MHz) using an acousto-optic modulator (AOM). Through the nonlinear light-atom interaction, this modulation was transferred into amplitude modulation on the 780 nm laser. This technique avoids background contamination [13] that would otherwise deteriorate the frequency discriminator signal.

Stabilization of the lasers' sum-frequency to the MTS discriminator signal was achieved by controlling the frequency of the 780 nm laser. The control loop bandwidth was 100 kHz, limited by the laser controller. This stabilization effectively compensated for the frequency fluctuations of the uncontrolled 776 nm laser (~5 MHz over 1000 s).

The frequencies of both lasers were compared to two modes of a commercial fiber frequency comb that was locked to a hydrogen maser. Each optical comb mode exhibited a frequency stability of $\approx 5 \times 10^{-13}$ at 1 s. The mixing products between the closest comb modes and the two lasers were separately measured on synchronously triggered counters. The sum-frequency was obtained by post processing the recorded beat notes.

The typical optical powers used to drive the two-photon transition were 3 and 4 μW for the 780 and 776 nm lasers, respectively. Even for these low powers, intensities within the fiber were large enough to produce substantial light shifts, thus the laser power coupled into the fiber were actively controlled. This was achieved by detecting the transmitted power of both lasers with a photomultiplier tube and photodiode, respectively. These signals were stabilized via attenuation of the corresponding AOM. Once stabilized, the light shift induced by each beam were investigated by varying the set point of each power control loop independently and monitoring the induced shift in the sum-frequency. The values obtained were 540 ± 20 kHz/μW and 29.7 ± 0.2 kHz/μW for the 780 and 776 nm beams, respectively. Using these measured light shift sensitivities, the frequency shifts and fluctuations calculated from the operating optical powers and residual fluctuations are presented in Table 1.

Table 1. Stability Limits at $\tau = 1$ s and Frequency Shifts

Physical Effect	Stability	Shift
Light-shifts:		
780 nm power	8×10^{-14}	1620 ± 60 kHz
776 nm power	3×10^{-14}	119 ± 1 kHz
776 nm frequency	1×10^{-14}	—
Alignment	1×10^{-11}	—
Rb–Rb collisions	$<1 \times 10^{-12}$	-1.8 ± 0.7 kHz
Magnetic field	1×10^{-12}	−960
Shot noise	1×10^{-13}	—
Electronic	$<1 \times 10^{-13}$	<130 kHz

The scale of the light shifts, measured above, depend on the detuning of both the 780 and 776 nm lasers from the intermediate state. Hence, uncontrolled frequency fluctuations of the 776 nm laser, and corresponding 780 nm corrections, cause additional light shifts. These shifts are proportional to $1/(\omega_{ij}^2 - \omega_l^2)$, where ω_{ij} is the transition frequency from level $|i\rangle$ to $|j\rangle$ and ω_l is the laser frequency. Using the measured drift of the 776 nm laser and the calibrated light shifts discussed above, an estimate of 10^{-14} stability is calculated for this noise source.

The measured fractional frequency stability of the stabilized sum-frequency is shown in Fig. 2. Also shown is the instability in the sum-frequency when both lasers are free-running. A stability of 9.8×10^{-12} was measured at an integration time of 1.3 s, which averaged down to a minimum of 5.9×10^{-12} at an integration time of ~10 s.

The dominant noise source was associated with alignment-driven coupling fluctuations of the lasers to the HC-PCF. Varying alignment of the input light modified the particular set of high-order optical modes that are excited within the fiber. Consequently, the mode

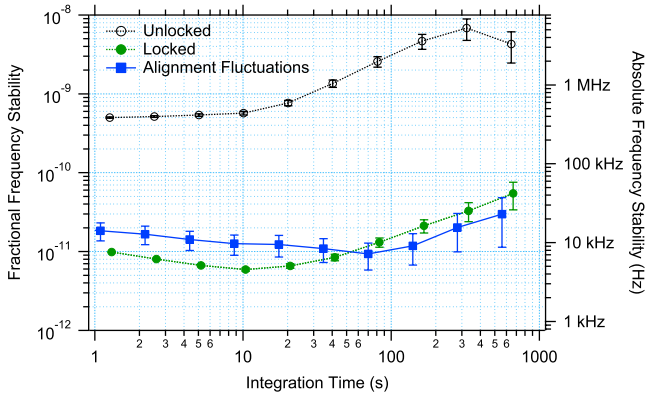

Fig. 2. Fractional frequency stability of the standard, when free-running and locked, and alignment fluctuation frequency noise.

shape and intensities are altered in the region where the 780 and 776 nm lasers overlap within the HC-PCF. These created varying light shifts that cannot be compensated for by simply controlling the overall power in the counterpropagating modes. An estimate of the frequency noise induced by this effect was made using a quadrant photodiode to measure the alignment fluctuations associated with movement of the HC-PCF within the vacuum system. Calibration of this motion, in terms of frequency shift, was made by displacing the in-coupling lens by a known amount and measuring the associated sum-frequency shift, which corresponded to 63 ± 15 kHz/μm. During this calibration the power control loops were engaged, eliminating overall power fluctuations as a cause of the frequency shifts. The resulting frequency noise estimate is within a factor of two of the measured stability, as shown in Fig. 2.

Frequency noise induced by collisional and magnetic field noise are negligible at current performance levels. At the operating system temperature (90 ± 5°C), Rb–Rb collisions produce frequency fluctuations and shifts [6], which are presented in Table 1. Shifts induced by magnetic fields were estimated by observing the two-photon transition while increasing the local magnetic field, yielding shifts of $\approx -1.8 \pm 1.0$ MHz/G. Hence, ambient magnetic field levels of ≈0.5 G with a noise of <1 mG caused a frequency shift of –960 kHz and noise of 10^{-12}.

Electronic and optical noise sources were investigated by monitoring the frequency error signal when detuned out of resonance with the two-photon transition. A limit of $\approx 10^{-13}$ fractional frequency stability was obtained originating from the shot-noise of the 780 nm light detected by the APD. These values demonstrate the potential stability achievable at this excitation level if the noise associated with fluctuating transverse mode structure within the HC-PCF could be eliminated.

A pathway for improvement is seen by removing optical mode fluctuations within the fiber. Similar alignment fluctuations have previously been reduced by more than an order of magnitude using active alignment systems [1]. The ultimate approach consists of loading Rb within an HC-PCF supporting only single mode guidance at 780 nm and sealing the fiber by splicing single mode fibers onto both ends. This approach removes both in-coupling alignment fluctuations along with the need of a vacuum system. This is a route for this platform to achieve frequency stabilities at the level of $\approx 10^{-13}$, which would match previously demonstrated Rb two-photon frequency standards [6] and begins to rival the stability of Rb fountain clocks [14] and hydrogen masers.

In conclusion, we demonstrate an optical frequency standard with a fractional frequency stability of 9.8×10^{-12} at a 1.3 s integration time. This standard is based on a two-photon two-color Doppler-free transition of a Rb vapor loaded within an HC-PCF, to which the sum-frequency of the two lasers stabilize. Stability was limited by optical mode shape changes within the fiber, driven by in-coupling alignment fluctuations. A route for improved stability is outlined, which should achieve $\approx 10^{-13}$ fractional frequency stability at integration times of 1 s. This architecture could lead to compact, robust, and efficient frequency standards.

The authors acknowledge financial support from the Australian Research Council under grants DP0877938, DE120102028, and FT0991631. We are grateful to Francois Couny for his contribution in fiber fabrication.

References

1. A. Lurie, F. N. Baynes, J. D. Anstie, P. S. Light, F. Benabid, T. M. Stace, and A. N. Luiten, Opt. Lett. **36**, 4776 (2011).
2. K. Knabe, S. Wu, J. Lim, K. A. Tillman, P. S. Light, N. Wheeler, F. Couny, R. Thapa, A. M. Jones, J. W. Nicholson, B. R. Washburn, F. Benabid, and K. L. Corwin, Opt. Express **17**, 16017 (2009).
3. S. Micalizio, C. E. Calosso, A. Godone, and F. Levi, Metrologia **49**, 425 (2012).
4. S. Knappe, V. Shah, P. D. D. Schwindt, L. Hollberg, J. Kitching, L.-A. Liew, and J. Moreland, Appl. Phys. Lett. **85**, 1460 (2004).
5. F. Esnault, N. Rossetto, D. Holleville, J. Delporte, and N. Dimarcq, Adv. Space Res. **47**, 854 (2011).
6. L. Hilico, R. Felder, D. Touahri, O. Acef, A. Clairon, and F. Biraben, Eur. Phys J. **4**, 219 (1998).
7. Y. Millerioux, D. Touahri, L. Hilico, A. Clairon, R. Felder, F. Biraben, and B. Debeauvoir, Opt. Commun. **108**, 91 (1994).
8. J. Bjorkholm and P. Liao, Phys. Rev. A **14**, 751 (1976).
9. D. Sheng, A. Pérez Galván, and L. Orozco, Phys. Rev. A **78**, 062506 (2008).
10. K. Saha, V. Venkataraman, P. Londero, and A. L. Gaeta, Phys. Rev. A **83**, 033833 (2011).
11. C. Perrella, P. Light, J. Anstie, T. M. Stace, F. Benabid, and A. Luiten, Phys. Rev. A **87**, 013818 (2013).
12. F. Couny, F. Benabid, and P. S. Light, Opt. Lett. **31**, 3574 (2006).
13. G. Camy, C. Bordé, and M. Ducloy, Opt. Commun. **41**, 325 (1982).
14. Y. Ovchinnikov and G. Marra, Metrologia **48**, 87 (2011).